Available online at www.sciencedirect.com
SCIENCE DIRECT®

International Journal of Mass Spectrometry 243 (2005) 257–268

International Journal of Mass Spectrometry
www.elsevier.com/locate/ijms

Gas-phase C–S bond cleavage and crown opening versus nitrogen heterocycle loss from Ru^{II} complex ions with 1,4,7,10-tetrathiacyclododecane and bidentate diimines

Raul A. Izquierdo[a], Cristina M.F. Barros[a], Francisco M.L. Amado[a], M. Graça O. Santana-Marques[a,*], A.J. Ferrer-Correia[a], J. Madureira[b], Teresa M. Santos[b], Vitor Félix[b]

[a] *Mass Spectrometry Laboratory, Department of Chemistry, University of Aveiro, 3810-193 Aveiro, Portugal*
[b] *CICECO, University of Aveiro 3810-193, Aveiro, Portugal*

Received 2 December 2004; accepted 23 March 2005
Available online 25 April 2005

Abstract

A new series of ruthenium(II) complexes with the general formula $[Ru^{II}([12]aneS_4)(NN)]X_2$, where NN are bidentate diimines, $[12]aneS_4$ is 1,4,7,10-tetrathiacyclododecane, and X is Cl^- or $PF_6{}^-$, were studied by electrospray mass spectrometry (ESMS). Thiacrown fragmentation and intact diimine loss are the two major types of gas-phase reactions observed. The diimine losses occur mainly from the ion pairs formed by the inner sphere cations with halogen anions and are more significant for the complexes with flexible cross-bridged diimines. The fragmentations occur predominantly without changes in the oxidation state of the metal centre.

Keywords: Ru(II) complexes; Diimines; $[12]aneS_4$; ESMS; Diimine loss; Thiacrown fragmentation

---

1. Introduction

Ruthenium(II) coordination compounds have been extensively evaluated for clinical applications, specially for the treatment of cancer. Their ligand exchange solution kinetics are similar to those of platinum(II) complexes, but ruthenium is unique among the platinum group in that the oxidation states Ru(II), Ru(III) and Ru(IV) are all accessible under physiological conditions. Moreover, ruthenium coordination compounds are less toxic than their platinum counterparts, as they have the ability to mimic iron in binding to biomolecules, such as serum transferrin and albumin, which are used by mammals to solubilise and transport iron, thereby reducing its toxicity [1]. Although it has been known for the past two decades that ruthenium(II) complexes with bidentate diimines, such as dipyrido[3,2-*a*:2′,3′-*c*]phenazine (dppz), form non-covalent adducts with DNA [2], the influence on adduct formation of factors such as shape and planarity of the diimine is the object of investigation to date [3,4] and novel Ru(II) compounds with diimine ligands, both mono- [5] and binuclear [6] are being synthesized up to now.

The synthesis, characterization and study of ruthenium(II) complexes with different potential intercalators of the diimine type and one common, non-intercalating ligand, such as a crown thioether, could clarify the mechanism of adduct formation of these type of compounds with DNA. We have, thus, synthesized and studied two series of heteroleptic ruthenium(II) octahedral complexes, $[Ru^{II}Cl[9]aneS_3)(NN)]X$ and $[Ru^{II}[12]aneS_4)(NN)]X_2$, where $[9]aneS_3$ and $[12]aneS_4$ are the thioethers, 1,4,7-trithiacyclononane and 1,4,7,10-tetrathiacyclododecane, respectively, NN are bidentate diimines, such as 2,2′-bipyridine (bpy), 1,10-phenanthroline (phen) and dipyrido[3,2-*a*:2′,3′-*c*]phenazine and X is Cl^- or $PF_6{}^-$ [7,8].

In a previous study by electrospray mass spectrometry (ESMS) of the first series of the heteroleptic ruthenium(II) octahedral complexes, we have found that the mass spectra of

---

[*] Corresponding author. Tel.: +351 234370696; fax: +351 234370084.
E-mail address: grmarques@dq.ua.pt (M.G.O. Santana-Marques).

1387-3806/$ – see front matter © 2005 Elsevier B.V. All rights reserved.
doi:10.1016/j.ijms.2005.03.008

all the $[Ru^{II}Cl[9]aneS_3)(NN)]X$ complexes were alike, and showed two peaks corresponding to losses of 64 and 92 Da ($HCl + CH_2CH_2$ and $HCl + 2CH_2CH_2$) from the inner sphere ions $[Ru^{II}Cl[9]aneS_3)(NN)]^+$. The formation of these diagnostic ions does not depend on the counter anion involved, occurs for a range of cone potential values, and proceeds mainly through C–S bond cleavages of the thiacrown, the dimines remaining attached to the metal centre [9].

Electrospray mass spectrometry has been increasingly used to study coordination complexes, since it was first applied to the homoleptic tris(2,2′-bipyridyne)ruthenium(II) and tris(1,10-phenanthroline)ruthenium(II) chlorides [10]. The advantages of the use of electrospray in the study of inorganic, organometallic and coordination compounds have been reported in several reviews [11–15]. Moreover, electrospray mass spectrometry/mass spectrometry (ESMS/MS) has provided a wealth of information on many aspects of metal complex gas-phase chemistry such as structure, binding energies, coordination geometry, type and donor groups of the ligands, among many others [16–38]. Collision-induced experiments have also been used combined with ion–molecule reactions to determine coordination numbers and to investigate ligand substitution in the gas-phase [39–41].

A significant number of coordination compounds exist as charged species in solution and can be transferred to the gas-phase, usually without changes both in their structure and their charge, although species that are not normally abundant in solution can be readily produced in the gas-phase. This is the case of the ion pairs formed under electrospray, for complexes of transition metals with strongly coordinating ligands, because the solution concentrations of such ion pairs are usually much lower than the solution concentrations of the inner sphere cations [16]. While for the complexes with $[9]aneS_3$ the inner sphere cations are singly charged, for the complexes with $[12]aneS_4$ they are doubly charged, thus having the ability of forming singly charged ion pairs with the counter anions.

In the present work, we report the study of the $[12]aneS_4$ complexes by ESMS and ESMS/MS. We found that the electrospray mass spectra of the complexes with $[12]aneS_4$ are strongly dependent on cone potential values, in contrast with the spectra of the complexes with $[9]aneS_3$. In addition, the gas-phase fragmentations of the complexes with $[12]aneS_4$ proceed not only through losses from the thiacrown, similar to those occurring for the $[9]aneS_3$ complexes, but also through intact NN nitrogen heterocycle loss.

2. Experimental

The synthesis and the characterization of the $[Ru^{II}([12]aneS_4)(NN)]X_2$ complexes (Fig. 1; Table 1) were published elsewhere [8]. All the complexes were characterized by elemental analysis, IR, ^1H NMR and UV–vis. The structures of the PF_6 salts of dip, dppz and dipa were determined by single crystal X-ray diffraction [8].

ESMS spectra were acquired with a Micromass Q-Tof 2 (Micromass, Manchester, UK), with a Z-spray source, an electrospray probe and a syringe pump. Source block and desolvation temperatures were 80 and 150 °C, respectively. The capillary voltage was 3000 V. The instrument was operated at a resolution of 9000 (50% valley). The spectra were acquired for a range of cone voltages (20–60 V) in order to obtain good signal-to-noise ratio for the ions of interest. Nitrogen was used as the nebulizer gas and argon as the collision gas. The samples were dissolved in methanol for the complexes with Cl^- as a counter ion and acetonitrile for the complexes with PF_6^-. Methanol was used as the eluent and the samples were introduced at a flow rate of $10\ \mu L\ min^{-1}$.

Collision-induced mass spectra (ESMS/MS) spectra were obtained by selecting the ion of interest with the quadrupole analyser and using the hexapole collision cell, for a range of collision energies from 20 to 40 eV.

3. Results

3.1. Mass spectra

The ion signals for the $[Ru^{II}([12]aneS_4)(NN)]X_2$ complexes are strongly dependent on cone potential values.

Table 1
Compounds studied and masses of the NN ligands and of the inner sphere complexes

Compounds $[Ru^{II}([12]aneS_4)(NN)]X_2$	NN ligands			Mass of the innersphere complexes[a] (Da) $[Ru^{II}([12]aneS_4)(NN)]^{2+}$
	Name	Abbreviation	Mass (Da)	
1	2,2′-Bipyridine	bpy	156	498
2	4,4′-Diphenyl-2,2′-bipyridine	dbp	308	650
3	1,10-Phenantroline	phen	180	522
4	5-Phenyl-1,10-phenantroline	5-phen	256	598
5	4-7′-Diphenyl-1,10-phenanthroline	dip	332	674
6	1,10-Phenantroline-5,6-dione	5,6-dione	210	552
7	Dipyrido[3,2-*a*:2′,3′-*c*]phenazine	dppz	282	624
8	9,10-Phenanthrenequinone diimine	phi	206	548
9	2,2′-Dipyridylmethane	dpm	170	512
10	2,2′-Dipyridylamine	dipa	171	513
11	2,2′-Dipyridylketone	dpk	184	526

[a] Monoisotopic mass (^{102}Ru).

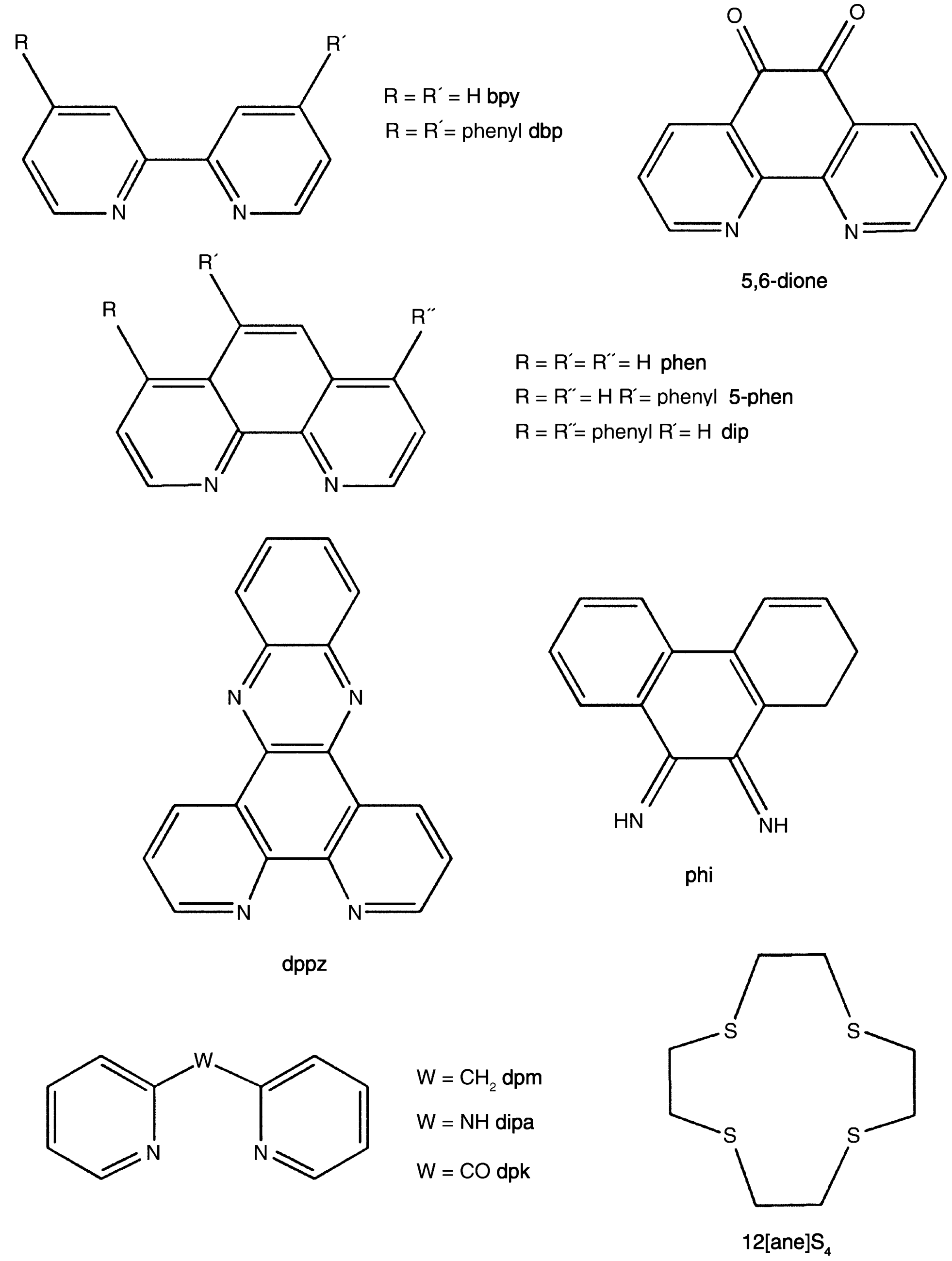

Fig. 1. Bidentate diimine ligands.

At lower values (20–30 V), we can observe the signals of the doubly charged $[Ru^{II}([12]aneS_4)(NN)]^{2+}$ ions (see Table 2), of the singly charged $[Ru^{II}([12]aneS_4\text{-}H)(NN)]^+$ ions, and also the signals of the doubly charged ions $[Ru^{II}([12]aneS_4\text{-}CH_2CH_2)(NN)]^{2+}$ formed by ethene loss from the crown through C–S bond cleavages, as well as the signals of the ion pairs formed by the inner sphere cations and the counter anions, $\{[Ru^{II}([12]aneS_4)(NN)]Cl\}^+$ and $\{[Ru^{II}([12]aneS_4)(NN)]PF_6\}^+$. The ion pair $\{[Ru^{II}([12]aneS_4)(NN)]F\}^+$ is also observed for the complexes where the counter ion is PF_6^-.

In general, as the cone voltage increases, the abundances of the doubly charged $[Ru^{II}([12]aneS_4)(NN)]^{2+}$ ions decrease. Other doubly charged ions such as $[Ru^{II}([12]aneS_4\text{-}2CH_2CH_2)(NN)]^{2+}$, $[Ru^{II}([12]aneS_4\text{-}3CH_2CH_2)(NN)]^{2+}$, $[Ru^{II}([12]aneS_4\text{-}2CH_2CH_2\text{-}S)(NN)]^{2+}$ and $[Ru^{II}([12]aneS_4\text{-}3CH_2CH_2\text{-}S\text{-}2H)(NN)]^{2+}$ are observed, as well as other singly charged species, such as the $[Ru^{II}([12]aneS_4\text{-}H\text{-}3CH_2CH_2\text{-}S)(NN)]^+$ ions and the protonated diimines, NNH^+. The ion pairs $\{[Ru^{II}([12]aneS_4)(NN)]Cl\}^+$, $\{[Ru^{II}([12]aneS_4)(NN)]F\}^+$ and $\{[Ru^{II}([12]aneS_4)(NN)]PF_6\}^+$ remain abundant with increasing cone voltages, whereas

Table 2
Precursor ions $[Ru^{II}([12]aneS_4)(NN)]^{2+}$, $\{[Ru^{II}([12]aneS_4)(NN)]Cl\}^{+}$, $[Ru^{II}([12]aneS_4\text{-}H)(NN)]^{+}$ and their product ions formed by crown fragmentation

Symbol	Ion formula	Mass loss (Da)
a	$[Ru([12]aneS_4)(NN)]^{2+}$	
a1	$[Ru([12]aneS_4\text{-}CH_2CH_2)(NN)]^{2+}$	28 from **a**
a2	$[Ru([12]aneS_4\text{-}2CH_2CH_2)(NN)]^{2+}$	56 from **a**
a3	$[Ru([12]aneS_4\text{-}3CH_2CH_2)(NN)]^{2+}$	84 from **a**
a4	$[Ru([12]aneS_4\text{-}2CH_2CH_2\text{-}S)(NN)]^{2+}$	88 from **a**
a5	$[Ru([12]aneS_4\text{-}3CH_2CH_2\text{-}S\text{-}2H)(NN)]^{2+}$	118 from **a**
b	$\{[Ru([12]aneS_4)(NN)]Cl\}^{+}$	
b1	$\{[Ru([12]aneS_4\text{-}CH_2CH_2)(NN)]Cl\}^{+}$	28 from **b**
b2	$\{[Ru([12]aneS_4\text{-}2CH_2CH_2)(NN)]Cl\}^{+}$	56 from **b**
b3	$\{[Ru([12]aneS_4\text{-}3CH_2CH_2)(NN)]Cl\}^{+}$	84 from **b**
c	$[Ru([12]aneS_4\text{-}H)(NN)]^{+}$	
c1	$[Ru([12]aneS_4\text{-}H\text{-}CH_2CH_2)(NN)]^{+}$	28 from **c**
c2	$[Ru([12]aneS_4\text{-}H\text{-}2CH_2CH_2)(NN)]^{+}$	56 from **c**
c3	$[Ru([12]aneS_4\text{-}H\text{-}3CH_2CH_2)(NN)]^{+}$	84 from **c**
c4	$[Ru([12]aneS_4\text{-}H\text{-}CH_2CH_2\text{-}SCHCH_2)(NN)]^{+}$	87 from **c**
c5	$[Ru([12]aneS_4\text{-}H\text{-}2CH_2CH_2\text{-}S)(NN)]^{+}$	88 from **c**
c6	$[Ru([12]aneS_4\text{-}H\text{-}2CH_2CH_2\text{-}S\text{-}2H)(NN)]^{+}$	90 from **c**
c7	$[Ru([12]aneS_4\text{-}4CH_2CH_2)(NN\text{-}H)]^{+}$	112 from **c**
c8	$[Ru([12]aneS_4\text{-}H\text{-}2CH_2CH_2\text{-}SCHCH_2)(NN)]^{+}$	115 from **c**
c9	$[Ru([12]aneS_4\text{-}H\text{-}3CH_2CH_2\text{-}S)(NN)]^{+}$	116 from **c**
c10	$[Ru([12]aneS_4\text{-}H\text{-}3CH_2CH_2\text{-}S\text{-}2H)(NN)]^{+}$	118 from **c**
c11	$[Ru([12]aneS_4\text{-}H\text{-}3CH_2CH_2\text{-}SCHCH_2)(NN)]^{+}$	143 from **c**
c12	$[Ru([12]aneS_4\text{-}H\text{-}3CH_2CH_2\text{-}2S)(NN)]^{+}$	148 from **c**
c13	$[Ru([12]aneS_4\text{-}H\text{-}3CH_2CH_2\text{-}2S\text{-}H)(NN)]^{+}$	149 from **c**
c14	$[Ru([12]aneS_4\text{-}H\text{-}2CH_2CH_2\text{-}3S\text{-}2H)(NN)]^{+}$	154 from **c**
c15	$[Ru([12]aneS_4\text{-}H\text{-}3CH_2CH_2\text{-}2S\text{-}CHCH)(NN)]^{+}$	174 from **c**

Table 3
Common product ions formed by diimine loss

Symbol	Ion formula	*m/z*
d	$[Ru([12]aneS_4)]^{2+}$	171 (mass 342)
d1	$[Ru([12]aneS_4)Cl(H_2O)]^{+}$	395
d2	$[Ru([12]aneS_4)Cl]^{+}$	377
d3	$[Ru([12]aneS_4\text{-}CH_2CH_2)Cl]^{+}$	349
d4	$[Ru([12]aneS_4\text{-}H)]^{+}$	341
d5	$Ru([12]aneS_4\text{-}CHCH_2)]^{+}$	315
d6	$Ru([12]aneS_4\text{-}H\text{-}CH_2CH_2)]^{+}$	313
d7	$Ru([12]aneS_4\text{-}H\text{-}CH_2CH_2\text{-}2H)]^{+}$	311
d8	$\{[Ru([12]aneS_4\text{-}2CH_2CH_2\text{-}S)]Cl\}^{+}$	289
d9	$[Ru([12]aneS_4\text{-}H\text{-}2CH_2CH_2)]^{+}$	285
d′1	$[Ru([12]aneS_4)F(H_2O)]^{+}$	379
d′2	$[Ru([12]aneS_4)F]^{+}$	361
d′3	$[Ru([12]aneS_4\text{-}CH_2CH_2)F]^{+}$	333
d′4	$[Ru([12]aneS_4\text{-}CH_2CH_2\text{-}2H)F]^{+}$	331

the abundances of the $[Ru^{II}([12]aneS_4\text{-}H)(NN)]^{+}$ ions decrease.

Ions with the same *m/z* values of the $[Ru^{II}([12]aneS_4\text{-}H\text{-}3CH_2CH_2\text{-}S)(NN)]^{+}$ ions were observed for the compounds, $[Ru^{II}Cl([9]aneS_3)(NN)]X$, with the same diimines[9]. In the case of the $[9]aneS_3$ compounds, these ions were formed by losses of HCl plus $2CH_2CH_2$ from the $[Ru^{II}Cl([9]aneS_3)(NN)]^{+}$ ions, as mentioned in Section 1. The proposed structure for the $[Ru^{II}([12]aneS_4\text{-}H\text{-}3CH_2CH_2\text{-}S)(NN)]^{+}$ ions is shown in Scheme 1.

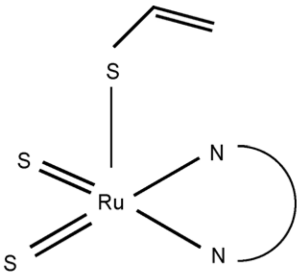

Scheme 1.

As the cone voltage further increases two different trends can be observed, respectively, for compounds **1–8** and **9–11**. At cone voltages of 40 V and above, the ion pairs are still abundant, the signals for the doubly charged ions are weak and for compounds **1–8**, the abundances of the singly charged ions $[Ru^{II}([12]aneS_4\text{-}H\text{-}3CH_2CH_2\text{-}S)(NN)]^{+}$ ions are higher, whereas for the second group, compounds **9–11**, intact diimine loss is an important process, forming the ions at *m/z* 395, $[Ru^{II}([12]aneS_4)Cl(H_2O)]^{+}$ (see Table 3); *m/z* 377, $[Ru^{II}([12]aneS_4)Cl]^{+}$; *m/z* 349, $[Ru^{II}([12]aneS_4\text{-}CH_2CH_2)Cl]^{+}$, when the counter ions are Cl^{-}, or the ions at *m/z* 379, $[Ru^{II}([12]aneS_4)F(H_2O)]^{+}$; *m/z* 361, $[Ru^{II}([12]aneS_4)F]^{+}$; *m/z* 333, $[Ru^{II}([12]aneS_4\text{-}CH_2CH_2)F]^{+}$, when the counter ions are PF_6^{-}, respectively.

Thus, at higher cone voltages the ions formed in the case of compounds **1–8** are mainly formed by cleavage of the $[12]aneS_4$ crown, the diimines remaining attached to the metal centre, whereas for the compounds **9–11** loss of the intact diimine is observed.

Methanol adduct ions were observed only for compounds **6** and **11**, both possessing non-coordinated carbonyl groups. When the counter ion was Cl^{-}, for compound **6,** with two uncoordinated carbonyl groups, adducts with one and two methanol molecules, $\{[Ru^{II}([12]aneS_4)(NN)](CH_3OH)\}^{2+}$ and $\{[Ru^{II}([12]aneS_4)(NN)](CH_3OH)_2\}^{2+}$, were observed as well as the corresponding ion pairs, $\{[Ru^{II}([12]aneS_4)(NN)]Cl(CH_3OH)\}^{+}$ and $\{[Ru^{II}([12]aneS_4)(NN)]Cl(CH_3OH)_2\}^{+}$, respectively, the species with one methanol being more abundant. Also, when the counter ion was Cl^{-}, for compound **11**, with one uncoordinated carbonyl group, the adducts $\{[Ru^{II}([12]aneS_4)(NN)](CH_3OH)\}^{2+}$ and $\{[Ru^{II}([12]aneS_4)(NN)]Cl(CH_3OH)\}^{+}$, were observed.

The species $\{[Ru^{II}([12]aneS_4)(NN)](CH_3OH)\}^{2+}$, $\{[Ru^{II}([12]aneS_4)(NN)](CH_3OH)_2\}^{2+}$, $\{[Ru^{II}([12]aneS_4)(NN)]F(CH_3OH)\}^{+}$ and $\{[Ru^{II}([12]aneS_4)(NN)]F(CH_3OH)_2\}^{+}$ were observed when the counter ion was PF_6^{-}, for compounds **11** and **6**, respectively.

3.2. MS/MS spectra

MS/MS spectra were obtained for the doubly charged $[Ru^{II}([12]aneS_4)(NN)]^{2+}$, for the ion pairs $\{[Ru^{II}([12]aneS_4)(NN)]Cl\}^{+}$, for the $[Ru^{II}([12]aneS_4\text{-}H)(NN)]^{+}$ ions as well as for the pentacoordinated ruthenium species, $[Ru^{II}([12]aneS_4\text{-}$

H-3CH_2CH_2-S)(NN)]$^+$. The MS/MS spectra were also obtained for the ion pairs {[Ru^{II}([12]aneS_4)(NN)]PF_6}$^+$ and {[Ru^{II}([12]aneS_4)(NN)]F}$^+$ as well as for the methanol adducts for compounds **6** and **11**. For each type of ions, the MS/MS spectra were acquired at the same cone voltages and collision energy values.

3.3. MS/MS spectra of the [Ru^{II}([12]aneS_4)(NN)]$^{2+}$ ions

The MS/MS spectra of the doubly charged ions [Ru^{II}([12]aneS_4)(NN)]$^{2+}$ show as the main fragment ions the doubly charged ions formed by losses from the crown, respectively, the [Ru^{II}([12]aneS_4-CH_2CH_2)(NN)]$^{2+}$, [Ru^{II}([12]aneS_4-2CH_2CH_2)(NN)]$^{2+}$, [Ru^{II}([12]aneS_4-3CH_2CH_2)(NN)]$^{2+}$, [Ru^{II}([12]aneS_4-2CH_2CH_2-S)(NN)]$^{2+}$ and [Ru^{II}([12]aneS_4-3CH_2CH_2-S-2H)(NN)]$^{2+}$ ions. For compounds **1**–**8**, a small peak corresponding to the singly charged [Ru^{II}([12]aneS_4-H-3CH_2CH_2-S)(NN)]$^+$ ion is also observed. For the compounds **1**, **2** and **8**–**11**, the singly charged protonated NNH$^+$ ions are formed, and also ions at *m/z* 313, [Ru^{II}([12]aneS_4-H-CH_2CH_2)]$^+$ and *m/z* 285, [Ru^{II}([12]aneS_4-H-2CH_2CH_2)]$^+$ formed by losses of the intact diimine plus fragments from the crown. The MS/MS spectra of the [Ru^{II}([12]aneS_4)(NN)]$^{2+}$ ions for compounds **1** (NN = bpy), **5** (NN = dip) and **9** (NN = dpm) are shown in Fig. 2.

3.4. MS/MS spectra of the ion pairs

The MS/MS spectra of the ion pairs with Cl^- and F^- are very similar, thus we will only describe the features of the spectra of the ion pairs with Cl^-. The MS/MS spectra of the {[Ru^{II}([12]aneS_4)(NN)]Cl}$^+$ ions show three different types of product ions. In the first type, the chloride ion and the diimine remain attached and the thiacrown fragments. This type includes the {[Ru^{II}([12]aneS_4-CH_2CH_2)(NN)]Cl}$^+$, the {[Ru^{II}([12]aneS_4-2CH_2CH_2)(NN)]Cl}$^+$ and the {[Ru^{II} ([12]aneS_4-3CH_2CH_2)(NN)]Cl}$^+$ ions. These ions are not very abundant and are not observed for the compounds **9**–**11**.

The second type corresponds to one chloride ion loss plus other losses from the crown, and is represented mainly by the [Ru^{II}([12]aneS_4-H)(NN)]$^+$, [Ru^{II}([12]aneS_4-H-2CH_2CH_2)(NN)]$^+$, [Ru^{II}([12]aneS_4-H-3CH_2CH_2)(NN)]$^+$ and [Ru^{II}([12]aneS_4-H-2CH_2CH_2-S)(NN)]$^+$ ions. In the case of compounds **9**–**11**, the [Ru^{II}([12]aneS_4-H)(NN)]$^+$ and [Ru^{II}([12]aneS_4-H-2CH_2CH_2)(NN)]$^+$ ions are observed,

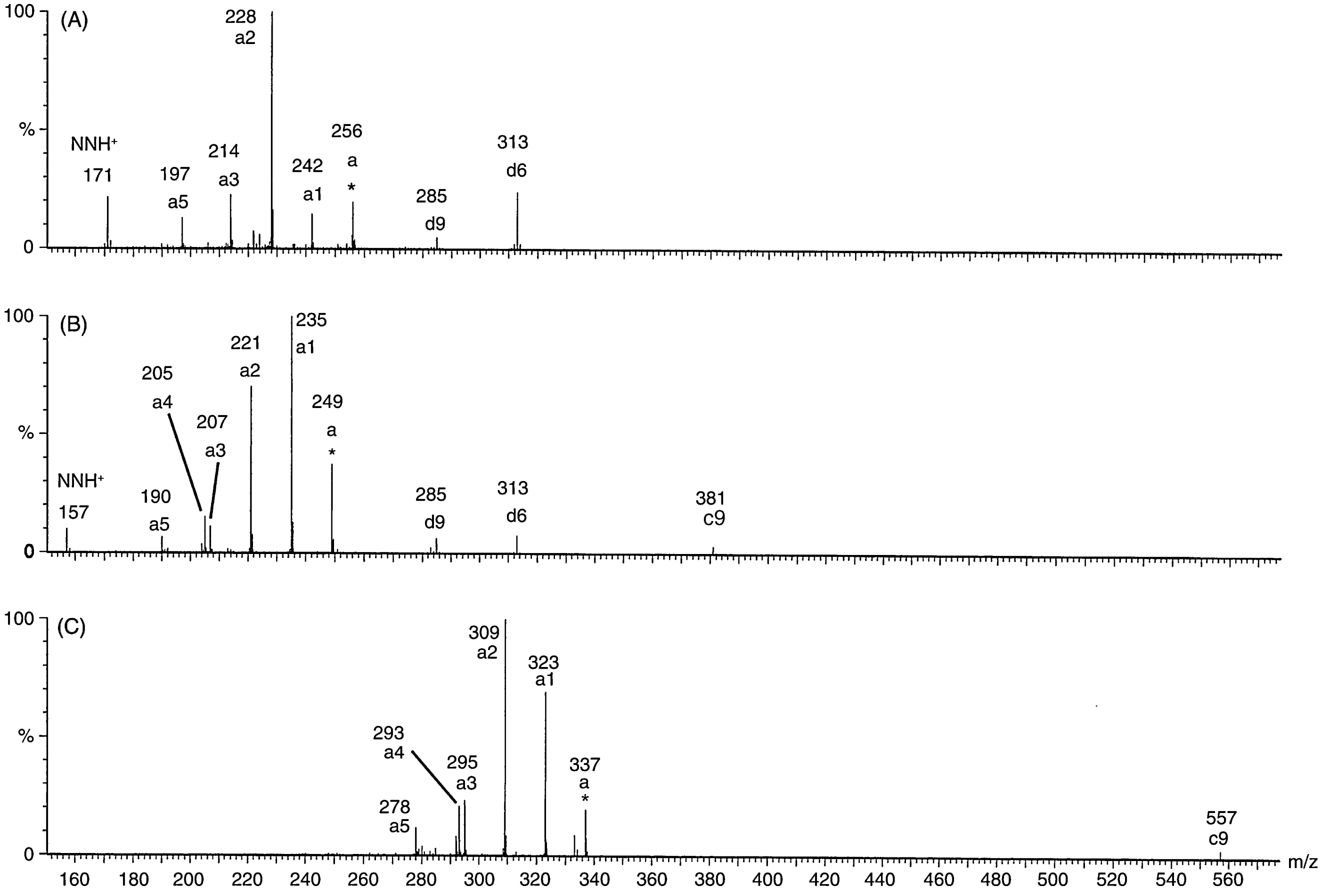

Fig. 2. ESMS/MS spectra of the [Ru^{II}([12]aneS_4)(NN)]$^{2+}$ ions: (A) compound **9**, (B) compound **1** and (C) compound **5**; (* and **a** = [Ru^{II}([12]aneS_4)(NN)]$^{2+}$, **a1** = [Ru^{II}([12]aneS_4-CH_2CH_2)(NN)]$^{2+}$, **a2** = [Ru^{II}([12]aneS_4-2CH_2CH_2)(NN)]$^{2+}$, **a3** = [Ru^{II}([12]aneS_4-3CH_2CH_2(NN)]$^{2+}$, **a4** = [Ru^{II}([12]aneS_4-2CH_2CH_2-S)(NN)]$^{2+}$, **a5** = [Ru^{II}([12]aneS_4-3CH_2CH_2-S-2H)(NN)]$^{2+}$, **c9** = [Ru^{II}([12]aneS_4-H-3CH_2CH_2-S)(NN)]$^+$, **d6** = [Ru^{II}([12]aneS_4-H-CH_2CH_2)]$^+$ and **d9** = [Ru^{II}([12]aneS_4-H-2CH_2CH_2)]$^+$).

whereas the $[Ru^{II}([12]aneS_4\text{-}H)(NN)]^+$ ion is not observed for the compounds **1–8,** but instead the NNH^+ ions are.

In the third type, the chloride ion remains attached, but the diimine is lost. This group includes the $[Ru^{II}([12]aneS_4)Cl(H_2O)]^+$, $[Ru^{II}([12]aneS_4)Cl]^+$ and $[Ru^{II}([12]aneS_4\text{-}CH_2CH_2)Cl]^+$, when the counter ions are Cl^-, which were also observed with high abundances at higher cone voltages in the mass spectra of compounds **9–11**.

The MS/MS spectra of the ion pairs with PF_6^-, $\{[Ru^{II}([12]aneS_4)(NN)]PF_6\}^+$ show as the only significant feature, one peak formed by loss of PF_5, the corresponding ion $\{[Ru^{II}([12]aneS_4)(NN)]F\}^+$, being very abundant.

The MS/MS spectra of the ion pairs $\{[Ru^{II}([12]aneS_4)(NN)]Cl\}^+$, for compounds **2**, (NN = dbp), **4** (NN = 5-phen) and **10** (NN = dipa) are shown in Fig. 3.

3.5. *MS/MS spectra of the $[Ru^{II}([12]aneS_4\text{-}H)(NN)]^+$ ions*

The $[Ru([12]aneS_4\text{-}H)(NN)]^+$ ions fragment through one and two ethene losses from the crown with formation of the $[Ru^{II}([12]aneS_4\text{-}H\text{-}CH_2CH_2)(NN)]^+$ and the $[Ru^{II}([12]aneS_4\text{-}H\text{-}2CH_2CH_2)(NN)]^+$ ions, although for compounds **1–8** these ions are not very abundant. The ions $[Ru^{II}([12]aneS_4\text{-}H\text{-}CH_2CH_2\text{-}SCHCH_2)(NN)]^+$ are formed for all the compounds, whereas the ions $[Ru^{II}([12]aneS_4\text{-}H\text{-}2CH_2CH_2\text{-}S\text{-}2H)(NN)]^+$ are formed with high abundances only for compounds **1–8**. Losses of the diimines plus losses from the crown lead to the ions at *m/z* 341, $[Ru^{II}([12]aneS_4\text{-}H)]^+$ and *m/z* 313, $[Ru^{II}([12]aneS_4\text{-}H\text{-}CH_2CH_2)]^+$, although these are only formed with high abundances for compounds **9–11**. The ions $[Ru^{II}([12]aneS_4\text{-}H\text{-}2CH_2CH_2\text{-}SCHCH_2)(NN)]^+$ and $[Ru^{II}([12]aneS_4\text{-}H\text{-}3CH_2CH_2\text{-}S)(NN)]^+$ are mostly formed for compounds **1–8**, whereas the ions $[Ru^{II}([12]aneS_4\text{-}H\text{-}3CH_2CH_2\text{-}SCHCH_2)(NN)]^+$, $[Ru^{II}([12]aneS_4\text{-}H\text{-}3CH_2CH_2\text{-}2S)(NN)]^+$, $[Ru^{II}([12]aneS_4\text{-}H\text{-}3CH_2CH_2\text{-}2S\text{-}H)(NN)]^+$, $[Ru^{II}([12]aneS_4\text{-}H\text{-}2CH_2CH_2\text{-}3S\text{-}2H)(NN)]^+$ and $[Ru^{II}([12]aneS_4\text{-}H\text{-}3CH_2CH_2\text{-}2S\text{-}CHCH)(NN)]^+$ (see Table 2) are only formed with high abundances for the compounds **3–8**.

The MS/MS spectrum of the $[Ru^{II}([12]aneS_4\text{-}H)(NN)]^+$ ions for compounds **1** (NN = bpy), **6** (NN = 5,6-dione) and **9** (NN = dpm) are shown in Fig. 4.

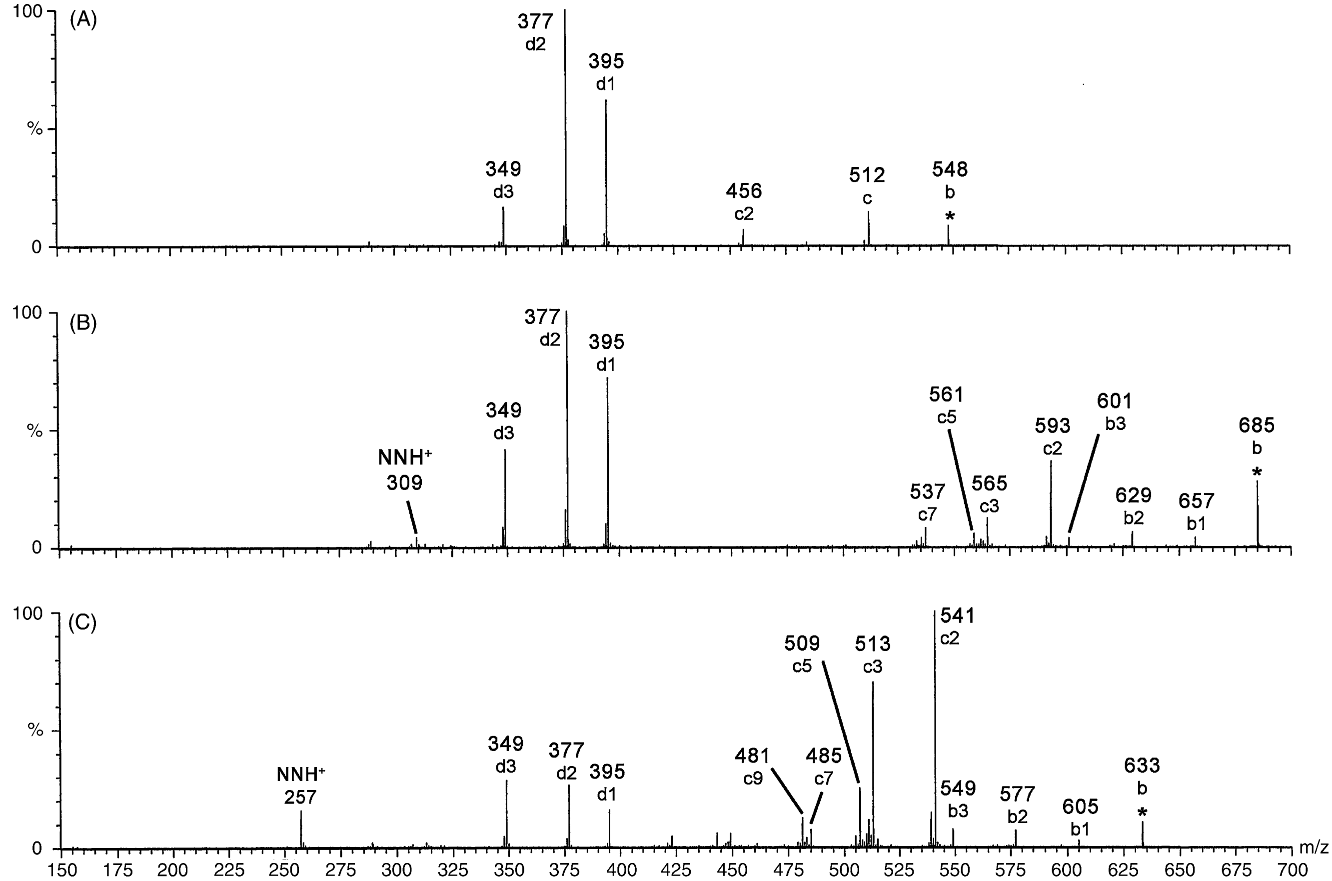

Fig. 3. ESMS/MS spectra of the ion pairs $\{[Ru^{II}([12]aneS_4)(NN)]Cl\}^+$: (A) compound **10**, (B) compound **2** and (C) compound **4**; (* and **b** = $\{[Ru^{II}([12]aneS_4)(NN)]Cl\}^+$, **b1** = $\{[Ru^{II}([12]aneS_4\text{-}CH_2CH_2)(NN)]Cl\}^+$, **b2** = $\{[Ru^{II}([12]aneS_4\text{-}2CH_2CH_2)(NN)]Cl\}^+$, **b3** = $\{[Ru^{II}([12]aneS_4\text{-}3CH_2CH_2(NN)]Cl\}^+$, **C** = $[Ru^{II}([12]aneS_4\text{-}H(NN)]^+$, **c2** = $[Ru^{II}([12]aneS_4\text{-}H\text{-}2CH_2CH_2)(NN)]^+$, **c3** = $[Ru^{II}([12]aneS_4\text{-}H\text{-}3CH_2CH_2)(NN)]^+$, **c5** = $[Ru^{II}([12]aneS_4\text{-}H\text{-}2CH_2CH_2\text{-}S)(NN)]^+$, **c7** = $[Ru^{II}([12]aneS_4\text{-}4CH_2CH_2)(NN\text{-}H)]^+$, **c9** = $[Ru^{II}([12]aneS_4\text{-}H\text{-}3CH_2CH_2\text{-}S)(NN)]^+$, **d1** = $[Ru^{II}([12]aneS_4)Cl(H_2O)]^+$, **d2** = $[Ru^{II}([12]aneS_4)Cl]^+$ and **d3** = $[Ru^{II}([12]aneS_4\text{-}CH_2CH_2)Cl]^+$).

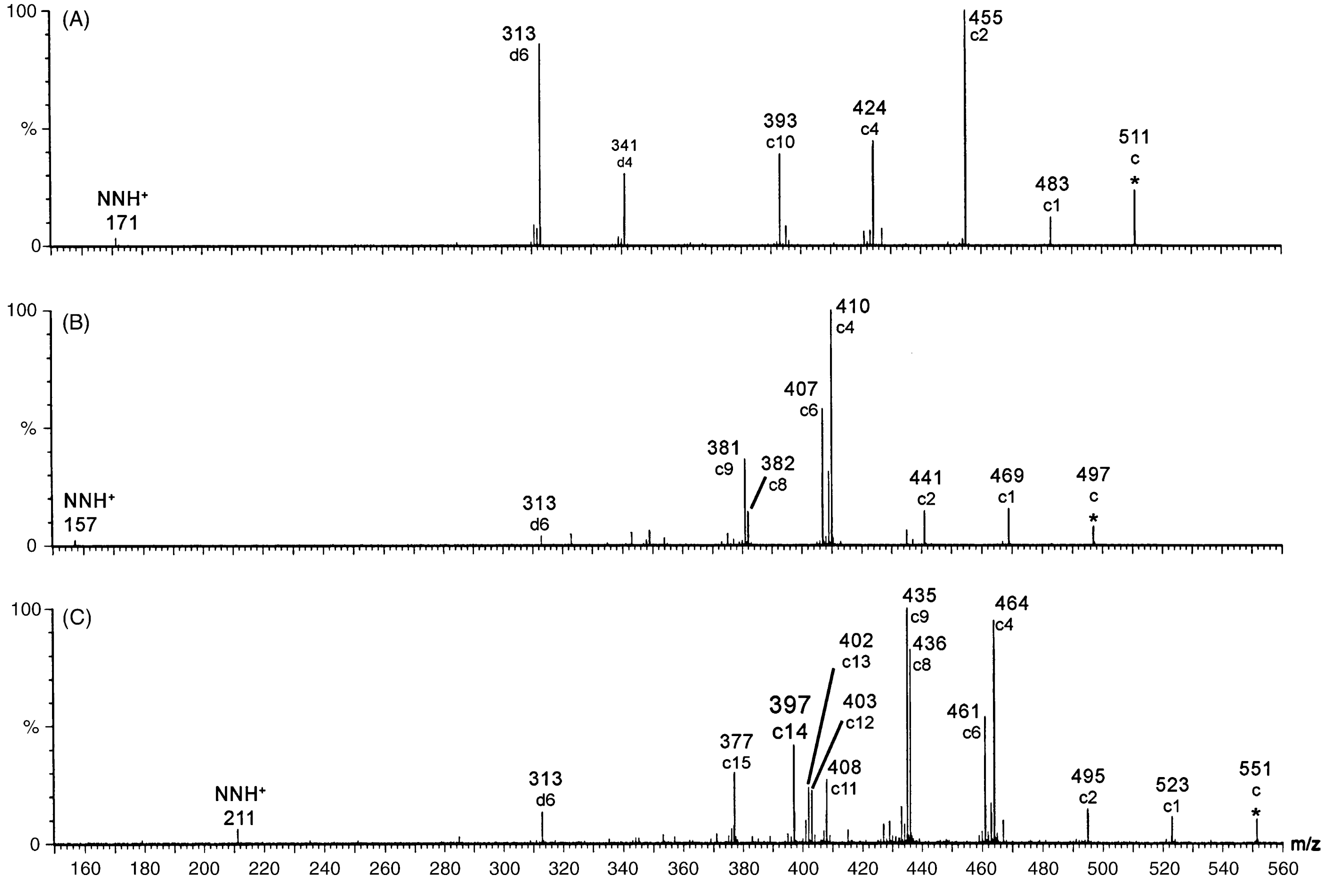

Fig. 4. ESMS/MS spectra of the $[Ru^{II}([12]aneS_4\text{-}H)(NN)]^+$ ions: (A) compound **9**, (B) compound **1** and (C) compound **6**; (* and **c** = $[Ru^{II}([12]aneS_4\text{-}H)(NN)]^+$ ions, **c1** = $[Ru^{II}([12]aneS_4\text{-}H\text{-}CH_2CH_2)(NN)]^+$, **c2** = $[Ru^{II}([12]aneS_4\text{-}H\text{-}2CH_2CH_2)(NN)]^+$, **c4** = $[Ru^{II}([12]aneS_4\text{-}H\text{-}CH_2CH_2\text{-}SCHCH_2)(NN)]^+$, **c6** = $[Ru^{II}([12]aneS_4\text{-}H\text{-}2CH_2CH_2\text{-}S\text{-}2H)(NN)]^+$, **c8** = $[Ru^{II}([12]aneS_4\text{-}H\text{-}2CH_2CH_2\text{-}SCHCH_2)(NN)]^+$, **c9** = $[Ru^{II}([12]aneS_4\text{-}H\text{-}3CH_2CH_2\text{-}S)(NN)]^+$, **c10** = $[Ru^{II}([12]aneS_4\text{-}H\text{-}3CH_2CH_2\text{-}S\text{-}2H)(NN)]^+$, **c11** = $[Ru^{II}([12]aneS_4\text{-}H\text{-}3CH_2CH_2\text{-}SCHCH_2)(NN)]^+$, **c12** = $[Ru^{II}([12]aneS_4\text{-}H\text{-}3CH_2CH_2\text{-}2S)(NN)]^+$, **c13** = $[Ru^{II}([12]aneS_4\text{-}H\text{-}3CH_2CH_2\text{-}2S\text{-}H)(NN)]^+$, **c14** = $[Ru^{II}([12]aneS_4\text{-}H\text{-}3CH_2CH_2\text{-}3S\text{-}2H)(NN)]^+$, **c15** = $[Ru^{II}([12]aneS_4\text{-}H\text{-}3CH_2CH_2\text{-}2S\text{-}CHCH)(NN)]^+$, **d4** = $[Ru^{II}([12]aneS_4\text{-}H)]^+$ and **d6** = $[Ru^{II}([12]aneS_4\text{-}H\text{-}CH_2CH_2)]^+$).

3.6. MS/MS spectra of the $[Ru^{II}([12]aneS_4\text{-}H\text{-}3CH_2CH_2\text{-}S)(NN)]^+$ ions

The MS/MS spectrum of the $[Ru^{II}([12]aneS_4\text{-}H\text{-}3CH_2CH_2\text{-}S)(NN)]^+$ ions show product ions corresponding to losses of HS, 2HS and S–CH=CH$_2$. The protonated nitrogen ligand NNH$^+$ is the most abundant product ion.

In Fig. 5A, the MS/MS spectrum of the $[Ru^{II}([12]aneS_4\text{-}H\text{-}3CH_2CH_2\text{-}S)(NN)]^+$ ions for compound **1** (NN = bpy) is shown and in Fig. 5B, the MS/MS spectrum of the ions with the same *m/z* value, 381, of the corresponding $[Ru^{II}([9]aneS_3\text{-}H\text{-}2CH_2CH_2)(NN)]^+$ ion (NN = bpy) is also shown. The spectra are identical, thus confirming that the ions are the same for the compounds of both [12]aneS$_4$ and [9]aneS$_3$ with the same diimines.

3.7. MS/MS spectra of the methanol adduct ions

The MS/MS spectra of the $\{[Ru^{II}([12]aneS_4)(NN)]Cl(CH_3OH)\}^+$ and $\{[Ru^{II}([12]aneS_4)(NN)]F(CH_3OH)\}^+$ ions on one hand, and of the $\{[Ru^{II}([12]aneS_4)(NN)]Cl(CH_3OH)_2\}^+$ and $\{[Ru^{II}([12]aneS_4)(NN)]F(CH_3OH)_2\}^+$, on the other hand, are very similar. The adducts with two methanol molecules are only formed in the case of compound **6** (NN = 5,6-dione), whereas the adducts with one methanol molecule are formed for both the compounds **6** and **11** (NN = dpk).

The MS/MS spectra of the $\{[Ru^{II}([12]aneS_4)(NN)]Cl(CH_3OH)\}^+$, $\{[Ru^{II}([12]aneS_4)(NN)]F(CH_3OH)\}^+$, $\{[Ru^{II}([12]aneS_4)(NN)]Cl(CH_3OH)_2\}^+$ and $\{[Ru^{II}([12]aneS_4)(NN)]F(CH_3OH)_2\}^+$ ions show different groups of product ions. In the first group, the dominant process is loss of the diimines with formation of the ions $[Ru^{II}([12]aneS_4)F(H_2O)]^+$, $[Ru^{II}([12]aneS_4)F]^+$, $[Ru^{II}([12]aneS_4\text{-}CH_2CH_2)F]^+$ and $[Ru^{II}([12]aneS_4\text{-}CH_2CH_2\text{-}2H)F]^+$ in the case of the adducts containing the fluoride ion, or the $[Ru^{II}([12]aneS_4)Cl(H_2O)]^+$, $[Ru^{II}([12]aneS_4)Cl]^+$ and $[Ru^{II}([12]aneS_4\text{-}CH_2CH_2)Cl]^+$ ions in the case of the adducts containing the chloride ion. The $[Ru^{II}([12]aneS_4\text{-}H\text{-}CH_2CH_2)]^+$ ions are formed for all the precursors (Table 3).

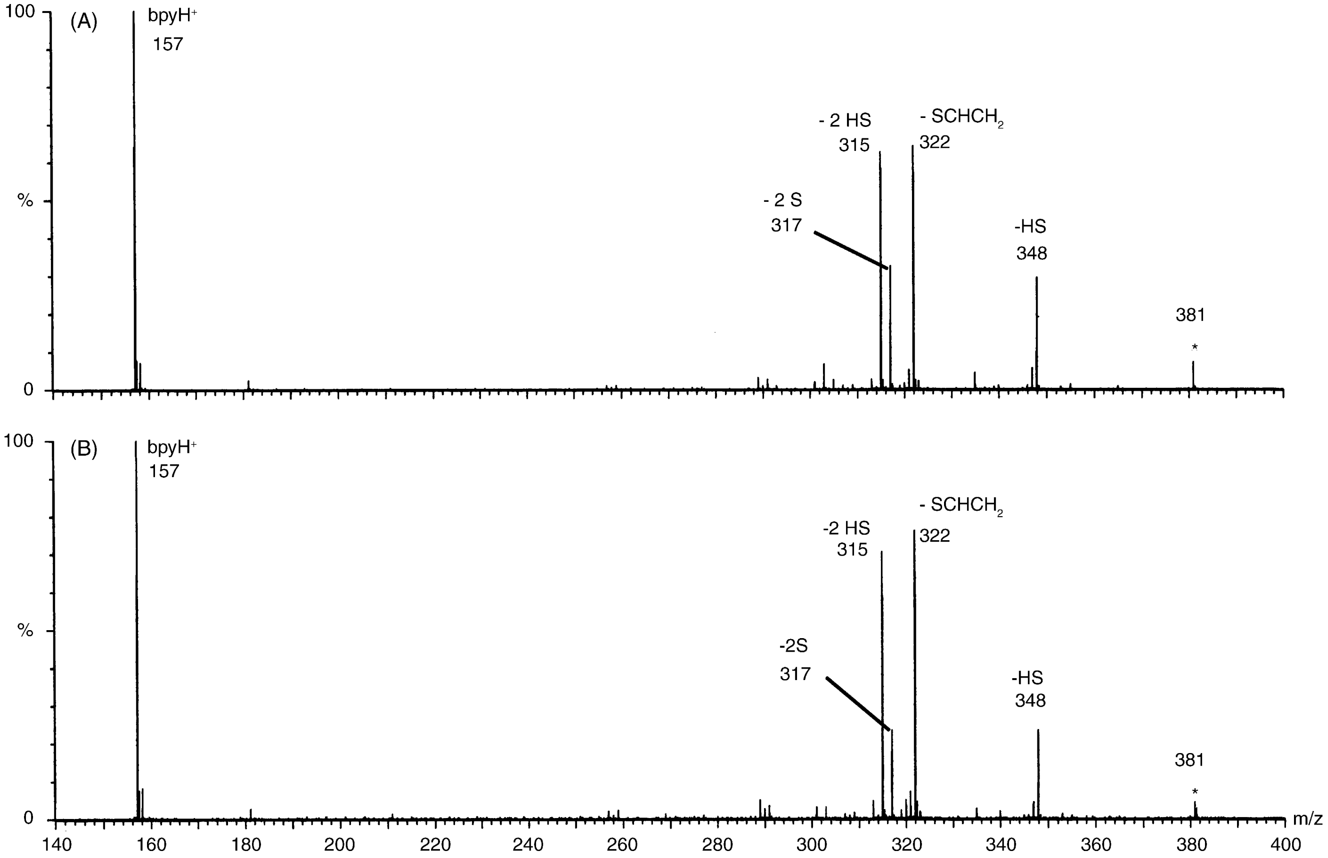

Fig. 5. ESMS/MS spectra of the ion of *m/z* 381: (A) the $[Ru^{II}([12]aneS_4\text{-}H\text{-}2CH_2CH_2\text{-}S(bpy)]$ ions and (B) the $[Ru^{II}([9]aneS_3\text{-}H\text{-}2CH_2CH_2(bpy)]$ ions.

In the second group, the ions are formed by counter ion loss and crown fragmentation, the methanol remaining attached. The main product ions of the precursor ion adducts with one methanol molecule are the $\{[Ru^{II}([12]aneS_4\text{-}H\text{-}2CH_2CH_2)(NN)](CH_3OH)\}^+$ and $\{[Ru^{II}([12]aneS_4\text{-}H\text{-}3CH_2CH_2)(NN)](CH_3OH)\}^+$ ions, formed by loss of HF or HCl plus two and three ethene molecules, and the $\{[Ru^{II}([12]aneS_4\text{-}H\text{-}2CH_2CH_2\text{-}S\text{-}2H)(NN)](CH_3OH)\}^+$ ions, formed by loss of HF or HCl plus other losses from the crown. The main product ions of the precursors with two methanol molecules are the $\{[Ru^{II}([12]aneS_4\text{-}H\text{-}2CH_2CH_2)(NN)](CH_3OH)_2\}^+$, $\{[Ru^{II}\text{-}([12]aneS_4\text{-}H\text{-}3CH_2CH_2)(NN)](CH_3OH)_2\}^+$ and the $\{[Ru^{II}\text{-}([12]aneS_4\text{-}H\text{-}2CH_2CH_2\text{-}S\text{-}2H)(NN)](CH_3OH)_2\}^+$ ions.

The third group is formed by product ions with low abundances but structurally significant. These are the proton bound species $[NNH(CH_3OH)]^+$ and $[NNH(CH_3OH)_2]^+$ for the precursor ions with two methanol molecules and the $[NNH(CH_3OH)]^+$for the precursor ions with one methanol molecule.

In Fig. 6 the MS/MS spectra of the $\{[Ru^{II}([12]aneS_4)(NN)]Cl(CH_3OH)\}^+$, $\{[Ru^{II}([12]aneS_4)(NN)]F(CH_3OH)\}^+$ and $\{[Ru^{II}([12]aneS_4)(NN)]Cl(CH_3OH)_2\}^+$ ions for compound **6** (NN = 5,6-dione) are shown.

4. Discussion

It is apparent from the obtained data that diimine loss is a process that occurs mainly via ion pair formation. Although this loss can also be observed from the doubly charged inner sphere $[Ru^{II}([12]aneS_4)(NN)]^{2+}$ ions and from the $[Ru^{II}([12]aneS_4\text{-}H)(NN)]^+$ ions, it occurs together with thiacrown fragmentation. The ions at *m/z* 395, $[Ru^{II}([12]aneS_4)Cl(H_2O)]^+$; *m/z* 377, $[Ru^{II}([12]aneS_4)Cl]^+$; *m/z* 349, $[Ru^{II}([12]aneS_4\text{-}CH_2CH_2)Cl]^+$, or the corresponding ions at *m/z* 379, $[Ru^{II}([12]aneS_4)F(H_2O)]^+$; *m/z* 361, $[Ru^{II}([12]aneS_4)F]^+$; *m/z* 333, $[Ru^{II}([12]aneS_4\text{-}CH_2CH_2)F]^+$, are only observed in the MS/MS spectra of the ion pairs $\{[Ru^{II}([12]aneS_4)(NN)]Cl\}^+$ or $\{[Ru^{II}([12]aneS_4)(NN)]F\}^+$. It is also apparent that diimine loss is more important in the case of the cross-bridged ligands dpm, dipa and dpk. These ligands form six-membered chelate rings, which are more flexible and less strongly coordinated due to loss of planarity, than the five-membered rings of the phen or even bpy compounds.

In a study by ESMS/MS of ion pairs of transition metal M^{2+} homoleptic compounds, $[M(phen)_3]ClO_4^+$ and $[M(bpy)_3]ClO_4^+$ (M = Mn, Fe, Co, Ni, Cu and Zn) has been reported that when formation of the $[M(phen)_2]ClO_4^+$

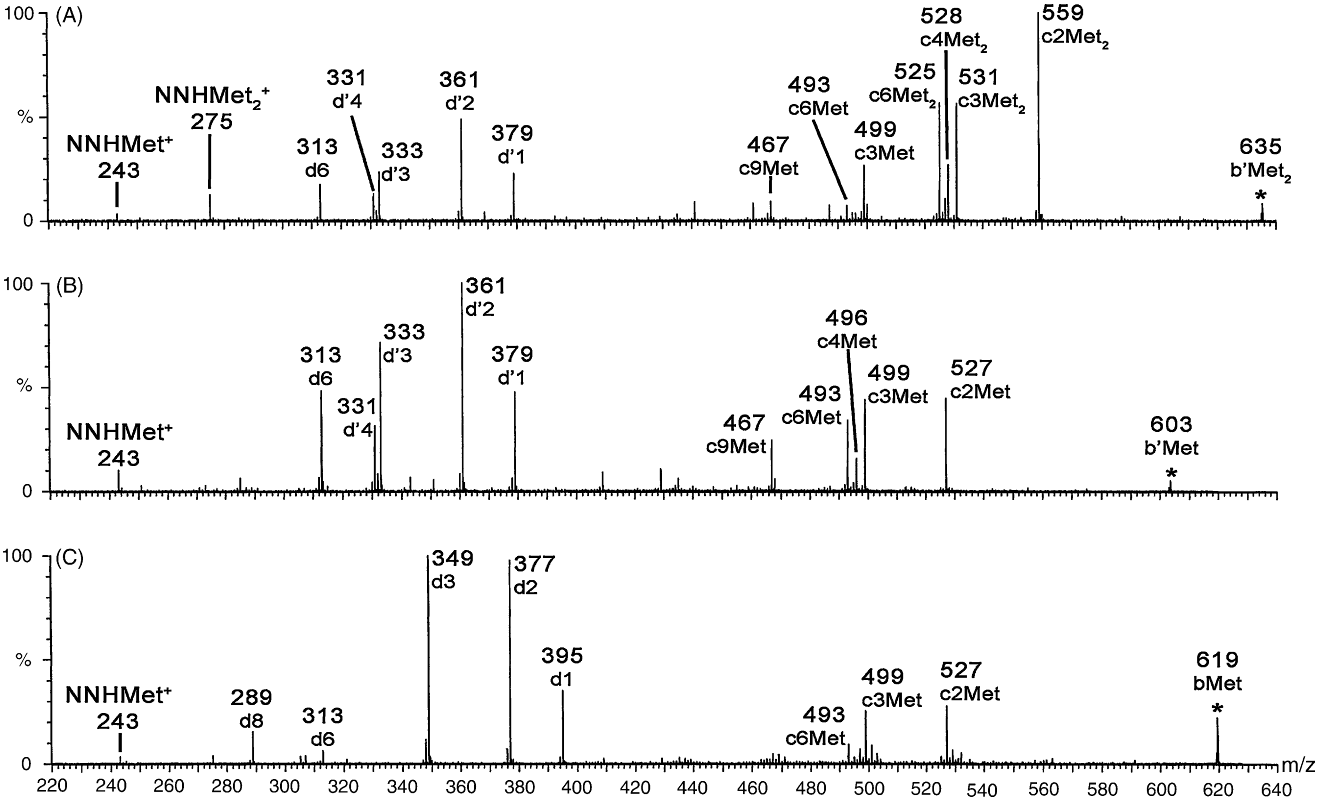

Fig. 6. ESMS/MS spectra of the methanol adducts of the ion pairs for compound **6**: (A) the $\{[Ru^{II}([12]aneS_4)(5,6\text{-dione})]F(CH_3OH)_2\}^+$ ions, (B) the $\{[Ru^{II}([12]aneS_4)(5,6\text{-dione})]F(CH_3OH)\}^+$ ions and (C) the $\{[Ru^{II}([12]aneS_4)(5,6\text{-dione})]Cl(CH_3OH)\}^+$ ions; (* and **bMet** = $\{[Ru^{II}([12]aneS_4)(5,6\text{-dione})]F(CH_3OH)_2\}^+$, * and **b′Met** = $\{[Ru^{II}([12]aneS_4)(5,6\text{-dione})]F(CH_3OH)\}^+$, * and **b′Met₂** = $\{[Ru^{II}([12]aneS_4)(5,6\text{-dione})]Cl(CH_3OH)\}^+$, **c2Met₂** = $\{[Ru^{II}([12]aneS_4\text{-H-}2CH_2CH_2)(5,6\text{-dione})](CH_3OH)_2\}^+$, **c3Met₂** = $\{[Ru^{II}([12]aneS_4\text{-H-}3CH_2CH_2)(5,6\text{-dione})](CH_3OH)_2\}^+$, **c4Met₂** = $\{[Ru^{II}([12]aneS_4\text{-H-}CH_2CH_2\text{-}SCHCH_2)(5,6\text{-dione})](CH_3OH)_2\}^+$, **c6Met₂** = $\{[Ru^{II}([12]aneS_4\text{-H-}2CH_2CH_2\text{-S-}2H)(5,6\text{-dione})](CH_3OH)_2\}^+$, **c2Met** = $\{[Ru^{II}([12]aneS_4\text{-H-}2CH_2CH_2)(5,6\text{-dione})](CH_3OH)\}^+$, **c3Met** = $\{[Ru^{II}([12]aneS_4\text{-H-}3CH_2CH_2)(5,6\text{-dione})](CH_3OH)\}^+$, **c4Met** = $\{[Ru^{II}([12]aneS_4\text{-H-}CH_2CH_2\text{-}SCHCH_2)(5,6\text{-dione})](CH_3OH)\}^+$, **c6Met** = $\{[Ru^{II}([12]aneS_4\text{-H-}2CH_2CH_2\text{-S-}2H)(5,6\text{-dione})](CH_3OH)\}^+$, **c9Met** = $\{[Ru^{II}([12]aneS_4\text{-H-}3CH_2CH_2\text{-S})(5,6\text{-dione})](CH_3OH)\}^+$, **d1** = $[Ru^{II}([12]aneS_4)Cl(H_2O)]^+$, **d2** = $[Ru^{II}([12]aneS_4)Cl]^+$, **d3** = $[Ru^{II}([12]aneS_4\text{-}CH_2CH_2)Cl]^+$, **d6** = $[Ru^{II}([12]aneS_4\text{-H-}CH_2CH_2)]^+$, **d8** = $[Ru^{II}([12]aneS_4\text{-}2CH_2CH_2\text{-S})]^+$, **d′1** = $[Ru^{II}([12]aneS_4)F(H_2O)]^+$, **d′2** = $[Ru^{II}([12]aneS_4)F]^+$, **d′3** = $[Ru^{II}([12]aneS_4\text{-}CH_2CH_2)F]^+$ and **d′4** = $[Ru^{II}([12]aneS_4\text{-}CH_2CH_2\text{-}2H)F]^+$).

or $[M(bpy)_2]ClO_4^+$ ions by collisional activation of the $[M(phen)_3]ClO_4^+$ and $[M(bpy)_3]ClO_4^+$ions through losses of phen or bpy, did occur, the counter anions remained in the outer sphere, interacting with the remaining phen and bpy ligands [16]. In the present case, the formation of the $[Ru^{II}([12]aneS_4)Cl]^+$ and $[Ru^{II}([12]aneS_4)F]^+$ ions from the ion pairs with the chloride and fluoride ions, respectively, probably involves transfer of the chloride and fluoride ions from the outer sphere to the inner sphere. A direct coordination of the halogen anions to the metal is expected to be stronger than the ion–dipole interaction between an outer sphere anion and the ligands.

The addition of one water molecule to the $[Ru^{II}([12]aneS_4)Cl]^+$ and $[Ru^{II}([12]aneS_4)F]^+$ with formation of the *m/z* 395, $[Ru^{II}([12]aneS_4)Cl(H_2O)]^+$ and *m/z* 379 $[Ru^{II}([12]aneS_4)F(H_2O)]^+$ ions with a coordination number of 6, reinforces the latter assumption. Addition of water to precursor ions in collision-induced experiments, in a hexapole collision cell, with argon, has been reported [31], the source of the associated water being, either the background gases or the argon itself. The argon is instrumental in the addition process, reducing the translational energies of the ions to which the water is added, to thermal or nearly thermal values [31]. In the present case, the water adds to the fragment ions $[Ru^{II}([12]aneS_4)Cl]^+$ and $[Ru^{II}([12]aneS_4)F]^+$ which constitutes evidence of the predominance of the NN ligand loss from the ion pairs.

Indirect evidence for coordination of halogen anions directly to the metal, is obtained from the ^1H NMR spectra of the $[Ru^{II}([12]aneS_4)(NN)]X_2$ complexes [8]. Broad lines for the aromatic protons closest to the ruthenium and for the thiacrown methylene protons suggest that chemical exchange occurs, probably with Ru-donor atom bond cleavage, to relieve steric crowding at the ruthenium centre [8]. If a similar process occurs in the gas-phase, incipient coordination of relatively small ions such as F^-, or even Cl^-, to the metal centre is possible. A subsequent loss of the diimine will give the $[Ru^{II}([12]aneS_4)Cl]^+$ and $[Ru^{II}([12]aneS_4)F]^+$ ions.

The formation of the $[Ru^{II}([12]aneS_4)(NN)]F^+$ ion pairs, as the only fragment ions, in the collision-induced dissoci-

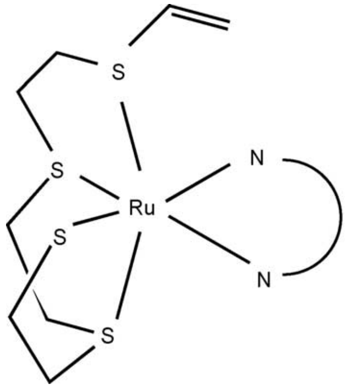

Scheme 2.

ation of the $\{[Ru^{II}([12]aneS_4)(NN)]PF_6\}^+$ ion pairs, reinforces the proposal of direct coordination of fluoride and chloride anions to the metal. The ion pairs with the PF_6^- counter ion fragment only through losses of PF_5, the PF_6^- counter ion, like the ClO_4^- [16] being too bulky for incipient coordination. Formation of ion pairs with fluoride, was observed under fast atom bombardment (FAB) [42,43] and both laser desorption (LD) and matrix assisted laser desorption (MALDI), for metal complexes, with PF_6^- as counter ions [44].

Losses of HX (X = anion) from the corresponding ion pairs of several metal complexes have been reported as occurring in collision-induced processes [30,45]. In the present case, formation of the $[Ru^{II}([12]aneS_4\text{-}H)(NN)]^+$ ions is observed, in the collision-induced decomposition of the ion pairs with the chloride and fluoride ions, only for compounds **9**–**11**. The $[Ru^{II}([12]aneS_4\text{-}H)(NN)]^+$ ions (Scheme 2) are formed through abstraction, by the counter ion, of one of the acidic methylene protons of the thiacrown, with crown opening and formation of a thienolate ion with conservation of the charge of the ruthenium centre. The steric crowding in this type of ions is still considerable, hence their higher abundance at lower cone voltages, and their formation under collision activation only for the complexes **9**–**11**, with more flexible ligands. Further thiacrown fragmentation either through the breaking of the more strained S–Ru bonds or through cleavage of other C–S bonds leads to ions such as $[Ru^{II}([12]aneS_4\text{-}H\text{-}CH_2CH_2)(NN)]^+$ and $[Ru^{II}([12]aneS_4\text{-}H\text{-}CH_2CH_2\text{-}SCH_2CH_2)(NN)]^+$, as can be observed in the collision-induced spectra of the $[Ru^{II}([12]aneS_4\text{-}H)(NN)]^+$ ions in Fig. 4.

Reduction of the metal centre was observed for metal complexes either in the electrospray source [46] or during collision-induced processes [19,20,24,25], and unusual charge states were observed in high-energy collision processes [47]. In the present case, the great majority of the singly charged species (not including the ion pairs and the fragment ions with an associated fluoride or chloride anion) can be rationalized as having a thienolate type structure. These ions may be formed through a migration of a methylene proton from the crown to the solvent, to the sulphur atom of the lost moiety, or to the NN ligand, thus possessing a ruthenium centre with a formal dipositive charge. The exceptions are the $[Ru^{II}([12]aneS_4\text{-}4CH_2CH_2)(NN\text{-}H)]^+$ ions (see Table 2 and Fig. 3B and C) and the $[Ru^{II}([12]aneS_4\text{-}H\text{-}3CH_2CH_2\text{-}S)(NN)]^+$ when formed in the gas-phase from the $[Ru^{II}([12]aneS_4)(NN)]^{2+}$ ions, as the corresponding charged moiety of the thiacrown was not detected in the MS/MS spectra.

The $[Ru^{II}([12]aneS_4\text{-}4CH_2CH_2)(NN\text{-}H)]^+$ ions are formed from the ion pairs with the chloride and fluoride ions, for complexes **1**–**8**, and although they are not very abundant, their formation shows that hydrogen loss, although not predominantly, occurs also from the diimines. Proton loss (or radical hydrogen loss followed by one electron reduction) was observed under FAB [48] and MALDI [44], for $[Ru^{II}(bpy)_3]X_2$ and $[Os^{II}(bpy)_3]X_2$ complexes, and a mechanism involving hydrogen loss from a unsaturated carbon, breaking of a nitrogen–metal bond, rotation of a pyridine ring and formation of a *ortho*-metallated complex through metal–carbon bond formation, was proposed to explain this loss [44]. Such a mechanism cannot be applied to compounds **3**–**7**, all of them having rigid, delocalised, π systems. Thus, we propose that the formation of the $[Ru^{II}([12]aneS_4\text{-}4CH_2CH_2)(NN\text{-}H)]^+$ ions occurs via a radical hydrogen loss plus one electron (possibly from the collision gas) reduction. The same may apply for the formation of the $[Ru^{II}([12]aneS_4\text{-}H\text{-}3CH_2CH_2\text{-}S)(NN)]^+$ in the gas-phase from the $[Ru^{II}([12]aneS_4)(NN)]^{2+}$ ions.

Ethene losses from the crown occur without changes of the overall charge, for both the doubly and singly charged ions. The elimination of ethene molecules is triggered by π backbonding of the ruthenium t_{2g} electrons to σ^* antibonding C–S orbitals [49–51].

There is a marked difference in the gas-phase behaviour of the $[Ru^{II}([12]aneS_4)(NN)]X_2$ complexes when compared to the gas-phase behaviour of the $[Ru^{II}Cl([9]aneS_3)(NN)]X$ complexes [9]. For the latter, two diagnostic ions, corresponding to the pentacoordinated ruthenium species, $[Ru^{II}([9]aneS_3\text{-}H\text{-}CH_2CH_2)(NN)]^+$ and $[Ru^{II}([9]aneS_3\text{-}H\text{-}2CH_2CH_2)(NN)]^+$, are formed for a wide range of cone voltages and the loss of the diimine is either not observed or originates ions with very weak signals. Moreover, for the $[Ru^{II}Cl([9]aneS_3)(NN)]X$ complexes, the diagnostic ions were even observed when the NN ligands were terpyridine and trispyrazolylmethane, potential tridentate ligands, acting as bidentate. For all the complexes with $[9]aneS_3$ the fragment ions are formed through losses from the crown, by abstraction of an acidic methylene proton by the chloride ligand, plus losses of ethene molecules, through C–S bond cleavages. Although, as it has been described above, the same type of processes occurs for the complexes with $[12]aneS_4$, for the latter, diimine loss also occurs, either as an in-source process (for a range of cone voltages) or in low energy collision-induced processes.

X-ray single crystal data for both groups of complexes show that they have distorted octahedral structures, the

[12]aneS_4 complexes being more distorted than the corresponding [9]aneS_3 complexes. For instance, for the ligand phen, the angles formed by the two equatorial sulphur atoms and the ruthenium centre, S_{equat}–Ru–S_{equat}, are 87.7° and 104.1°, for the complexes with the [9]aneS_3 and the [12]aneS_4 crowns, respectively. The differences between the angles formed by the atoms at opposite axial positions and the ruthenium centre are also significant, S_{axial}–Ru–Cl 178.8° and S_{axial}–Ru–S_{axial} 105.1°. The angles formed by the metal centre and the two nitrogen atoms, N–Ru–N, are 78.8° and 79.6°, respectively [7,8]. Although extrapolations from solid-phase, where we have to consider the overall packing arrangement, counter ions included, to gas-phase, where there may be changes in the coordination environment [52], must be done with caution, the increase of steric strain from the [9]aneS_3 to the [12]aneS_4 complexes, plus the absence of a negatively charged ligand in the inner sphere of the [12]aneS_4 complexes, are the probable causes of the dissimilar gas-phase behaviour of both groups of complexes.

An interesting similarity between the two groups of complexes is the formation of identical ions $[Ru^{II}S_2SCHCH_2(NN)]^+$ for both the [12]aneS_4 and the [9]aneS_3 complexes, as can be seen in Fig. 5. A square piramidal geometry with a pentacoordinated ruthenium (Scheme 1) has been proposed for the $[Ru^{II}S_2SCHCH_2(NN)]^+$ ion [40]. Square piramidal ruthenium(II) species, although not common, have been known since long [53] and, more recently, ruthenium(II) porphyrin complexes with carbonyl axial ligands have been studied by mass spectrometry [54]. The observed collision-induced losses, from the $[Ru^{II}S_2(SCHCH_2)(NN)]^+$ ion, of S–CH=CH_2, HS and 2HS (Fig. 5), will originate the species $[Ru^{II}S_2(NN)]^+$, $[Ru^{II}S(S{=}C{=}CH_2)(NN)]^+$ and $[Ru^{II}(S{-}C{\equiv}CH)(NN)]^+$, respectively.

Other interesting feature is related to the complexes **6** and **11**, with diimines containing carbonyl groups. Adducts with one and two methanol molecules of the ion pairs with the chloride and fluoride ions are observed. From observation of the collision-induced spectra of these adduct ions it is apparent that the bonds between the two diimines and the methanol molecules are stronger than the S–C and C–H bonds from the thiacrown, as several methanol adducts of ions such as the $[Ru^{II}([12]aneS_4\text{-}H\text{-}2CH_2CH_2)(NN)]^+$ and the $[Ru^{II}([12]aneS_4\text{-}3CH_2CH_2)(NN)]^+$ are observed (Fig. 6). The presence of $[Ru^{II}([12]aneS_4)Cl(H_2O)]^+$, $[Ru^{II}([12]aneS_4)Cl]^+$ and $[Ru^{II}([12]aneS_4\text{-}CH_2CH_2)Cl]^+$ ions (and their fluoride analogues) and of the less abundant, but structurally significant $NNHMet^+$ and $NNHMet_2{}^+$ ions (Met = CH_3OH), shows that the methanol molecules are bonded directly to the carbonyl groups, most likely through hydrogen bonds.

As an alternative explanation for the observed strong bonding between methanol and the two diimines, in the case of complexes **6** and **11**, we can consider the occurrence, in the source, of a chemical reaction, such as ketal formation. It has been reported recently, that storage of a methanolic solution of the compound $[Ru^{II}(dpk)(CO)_2Cl_2]$ in the dark, resulted in the addition of methanol to the coordinated dpk, with formation of a deprotonated ketal, the methoxydi(2-pyridyl)methoxide [55]. We are currently pursuing our studies on this subject.

5. Conclusions

For the $[Ru^{II}([12]aneS_4)(NN)]X_2$ complexes studied, thiacrown fragmentation and diimine loss are the two major types of gas-phase decomposition processes. The ions formed through diimine losses are more abundant for the complexes with the more flexible cross-bridged ligands, compounds **9–11**, and less abundant for the complexes with rigid delocalised π systems, compounds **3–8**. Diimine loss occurs mostly from the ion pairs with chloride and fluoride anions with probable coordination of the anions to the ruthenium centre. Conservation of the formal oxidation number of the metal centre is a predominant feature.

Acknowledgements

The authors wish to thank FCT (Fundação para a Ciência e Tecnologia) for financial support (POCTI/42883/QUI/2001). R.A. Izquierdo thanks the University of Aveiro for a Ph.D. scholarship.

References

[1] C.S. Allardyce, P.J. Dyson, Platinum Met. Rev. 45 (2001) 62.
[2] A.M. Pyle, J.P. Rehmann, R. Meshoyer, C.V. Kumar, N.J. Turro, J.K. Barton, J. Am. Chem Soc. 111 (1989) 3051.
[3] H. Xu, K.-C. Zheng, Y. Chen, Y.-Z. Li, L.-J. Lin, H. Li, P.-X. Zhang, L.-N. Ji, Dalton Trans. 11 (2003) 2260.
[4] Q.-L. Zhang, J.-H. Liu, J.-Z. Liu, P.-X. Zhang, X.-Z. Ren, Y. Liu, Y. Huang, L.-N. Ji, J. Inorg. Biochem. 98 (2004) 1405.
[5] G.-Y. Bai, K.-Z. Wang, Z.-M. Duan, L.-H. Gao, J. Inorg. Biochem. 98 (2004) 1017.
[6] J.-Z. Wu, L. Yuan, J. Inorg. Biochem. 98 (2004) 41.
[7] J. Madureira, T.M. Santos, B.J. Goodfellow, M. Lucena, J.P. Jesus, M.G. Santana-Marques, M.G.B. Drew, V. Felix, J. Chem. Soc., Dalton Trans. 23 (2000) 4422.
[8] T.M. Santos, B.J. Goodfellow, J. Madureira, J.P. Jesus, V. Felix, M.G.B. Drew, New J. Chem. 23 (1999) 1015.
[9] M.G.O. Santana-Marques, F.M.L. Amado, A.J. Ferrer Correia, M. Lucena, J. Madureira, B.J. Goodfellow, V. Felix, T.M. Santos, J. Mass Spectrom. 36 (2001) 529.
[10] V. Katta, S.K. Chowdhury, B.T. Chait, J. Am. Chem. Soc. 112 (1990) 5348.
[11] R. Colton, A. D'Agostino, J.C. Traeger, Mass Spectrom. Rev. 14 (1995) 79.
[12] C.L. Gatlin, F. Turecek, in: R.B. Cole (Ed.), Electrospray Ionization Mass Spectrometry: Fundamentals, Instrumentation and Applications, Wiley, New York, 1997, p. 527.
[13] W. Henderson, B.K. Nicholson, L.J. McCaffrey, Polyhedron 17 (1998) 4291.
[14] I.I. Stewart, Spectrochim. Acta, Part B 54 (1999) 1649.

[15] J.C. Traeger, Int. J. Mass Spectrom. 200 (2000) 387.
[16] R.W. Vachet, J.H. Callahan, J. Mass Spectrom. 35 (2000) 311.
[17] A.J. Canty, P.R. Traill, R. Colton, I.M. Thomas, Inorg. Chim. Acta 210 (1993) 91.
[18] T.-C. Lau, J. Wang, K.W.M. Siu, R. Guevremont, J. Chem. Soc., Chem. Commun. 12 (1994) 1487.
[19] C.L. Gatlin, F. Turecek, T. Vaisar, J. Mass Spectrom. 30 (1995) 1605.
[20] C.L. Gatlin, F. Turecek, T. Vaisar, J. Mass Spectrom. 30 (1995) 1627.
[21] C.L. Gatlin, F. Turecek, T. Vaisar, J. Am. Chem. Soc. 117 (1995) 3637.
[22] E. Alvarez, A. Wu, C. Liou, J. Brodbelt, J. Am. Chem. Soc. 118 (1996) 9131.
[23] R. Arakawa, G. Matsubayashi, N. Ohashi, S. Furuuchi, T. Matsuo, M.M. Ali, M. Haga, J. Mass Spectrom. 31 (1996) 861.
[24] T.-C. Lau, Z. Wu, J. Wang, K.W.M. Siu, R. Guevremont, Inorg. Chem. 35 (1996) 2169.
[25] M. Shahgoli, J.H. Callahan, B.J. Rappoli, D.A. Rowley, J. Mass Spectrom. 32 (1997) 1080.
[26] M. Kohler, J.A. Leary, J. Am. Soc. Mass Spectrom. 8 (1997) 1124.
[27] J. Shen, J. Brodbelt, Int. J. Mass Spectrom. 176 (1998) 39.
[28] J. Shen, J. Brodbelt, J. Am. Soc. Mass Spectrom. 10 (1999) 126.
[29] J. Shen, J. Brodbelt, J. Mass Spectrom. 34 (1999) 137.
[30] G. Smith, A. Kaffashan, J.A. Leary, Int. J. Mass Spectrom. 182–183 (1999) 299.
[31] C. Seto, J.A. Stone, Int. J. Mass Spectrom. 192 (1999) 289.
[32] F. Rogalewicz, Y. Hoppilliard, G. Ohanessian, Int. J. Mass Spectrom. 201 (2000) 307.
[33] Y. Hoppilliard, F. Rogalewicz, G. Ohanessian, Int. J. Mass Spectrom. 201 (2000) 267.
[34] S.P. Gaucher, J.A. Leary, Int. J. Mass Spectrom. 197 (2000) 139.
[35] D.A. Plattner, D. Feichtinger, J. El-Bahraoui, O. Wiest, Int. J. Mass Spectrom. 195–196 (2000) 351.
[36] H. Desaire, J. Leary, Int. J. Mass Spectrom. 209 (2001) 171.
[37] J.L. Seymour, F. Turecek, J. Mass Spectrom. 37 (2002) 533.
[38] A.L. Chaparro, R.W. Vachet, J. Mass Spectrom. 38 (2003) 333.
[39] R.W. Vachet, J.A.R. Hartman, J.H. Callahan, J. Mass Spectrom. 33 (1998) 1209.
[40] R.W. Vachet, J.R. Hartman, J.W. Gertner, J.H. Callahan, Int. J. Mass Spectrom. 204 (2001) 101.
[41] S. Wee, R.A.J. O'Hair, W.D. McFadyen, Rapid. Commun. Mass Spectrom. 18 (2004) 1221.
[42] G. Denti, S. Serroni, G. Sindona, N. Ucella, J. Am. Soc. Mass Spectrom. 4 (1993) 306.
[43] X. Liang, S. Suwanrumpha, R.B. Freas, Inorg. Chem. 30 (1991) 652.
[44] J.E. Ham, B. Durham, J.R. Scott, J. Am. Soc. Mass Spectrom. 14 (2003) 393.
[45] R.E. Shepherd, J.M. Slocik, T.W. Stringfield, K.V. Somayajula, A.A. Amoscato, Inorg. Chim. Acta 357 (2004) 965.
[46] H. Lavanant, H. Virelizier, Y. Hoppiliard, J. Am. Soc. Mass Spectrom. 9 (1998) 1217.
[47] A.B. Nielsen, P. Hvelplund, S.T. Nielsen, Int. J. Mass Spectrom. 232 (2004) 79.
[48] R.L. Cerny, B.P. Sullivan, M.M. Bursey, T.J. Meyer, Inorg. Chem. 24 (1985) 397.
[49] A.J. Blake, A.J. Holder, T.I. Hyde, H.-J. Kuppers, M. Schroder, S. Stotzel, K. Wieghardt, J. Chem. Soc., Chem. Commun. 21 (1989) 1600.
[50] G.E.D. Mullen, M.J. Went, S. Wocadlo, A.K. Powell, P.J. Blower, Angew. Chem. Int. Ed. Engl. 36 (1997) 1205.
[51] G.E.D. Mullen, T.F. Fassler, M.J. Went, K. Howland, B. Stein, P.J. Blower, J. Chem. Soc., Dalton Trans. 21 (1999) 3759.
[52] J.A.R. Hartman, A.L. Kammier, R.J. Spracklin, W.H. Pearson, M.Y. Combariza, R.W. Vachet, Inorg. Chim. Acta 357 (2004) 1141.
[53] E.A. Seddon, K.R. Seddon, in: R.J.H. Clark (Ed.), The Chemistry of Ruthenium, Topics in Inorganic and General Chemistry, Elsevier, Amsterdam, 1984, p. 588.
[54] M. Frauenkron, A. Berkesssel, J.H. Gross, Eur. Mass Spectrom. 3 (1997) 427.
[55] L. Spicia, G.B. Deacon, C.M. Kepert, Coord. Chem. Rev. 248 (2004) 1329.